

The effect of Fe on crystal structure and elasticity superhydrous Phase H under high pressure by First-principles calculations

Lei Liu¹, Longxing Yang¹, Guangshu Yang², Li Yi¹, Hong Liu¹, Xiaoyu Gu¹, Hanyu Wang¹, Chunqiang Zhuang^{*,3}

⁽¹⁾ United Laboratory of High-Pressure Physics and Earthquake Science, Institute of Earthquake Forecasting, Chinese Earthquake Administration, Beijing100036, China

⁽²⁾ Faculty of Land Resources Engineering, Kunming University of Science and Technology, Kunming 650093, Yunnan, China

⁽³⁾ Institute of Microstructure and Property of Advanced Materials, Beijing Key Lab of Microstructure and Property of Advanced Materials, Beijing University of Technology, Beijing100124, China

Article history: received November 25, 2019; accepted September 3, 2020

Abstract

Being one of the potentially important hydrous phases of the lower mantle, it is important to study the properties of phase H to understand the structure and composition of the mantle. The crystal structure, elastic modulus, and seismic wave velocity of phase H under different Fe concentrations (0, 12.5, 25, 100 at%) at 16–60 GPa were calculated by the first-principles simulation. The density of phase H linearly increases with increasing Fe concentration. The iron concentrations of 35.5–84.3 at% lead to densities matching the mantle density profile at different depths of the Earth. The effects of Fe on different elastic constants show varying tendencies. The K value increases with the Fe concentration, while the G value decreases. The values for V_p and V_s increase almost linearly with the rise in pressure. The V_p and V_s values decrease with increasing Fe content. The wave velocities of the pure-Mg phase H and Fe-bearing phase H are close to the typical velocity of the Earth at 500–1400 km depth. The FeOOH-AlOOH-MgSiH₂O₄-FeSiH₂O₄ system may be responsible for the observed seismic properties of LLSVP in the Earth's lower mantle. The quantitative effect of Fe on the density, elastic moduli (K and G), and wave velocities (V_p and V_s) are listed as fitted equations. These results help to infer the Fe concentration and structure of the deep Earth.

Keywords: Phase H; Fe; superhydrous phase; High pressure; First-principles simulation.

1. Introduction

Water plays an important role in the evolution and dynamics of Earth due to its strong influence on the physical and chemical characteristics of the Earth materials. The phase H and the solid solution formed by phase H with δ -phase AlOOH (phase H+ δ -AlOOH) are considered to be the most potential hydrous phases present under the deep lower mantle conditions [Ohtani et al., 2014; Ghosh and Schmidt, 2014; Nishi et al., 2018, 2019]. Iron is abundantly

found in the mantle, usually as the substitute for magnesium in mantle minerals. It was found that the incorporation of iron in silicate minerals modifies their crystal structures and physical properties [Liu et al., 2010; Tsuchiya and Tsuchiya, 2009; Higo et al., 2006; Hazen et al., 2000; Ganskow et al., 2010; Jacobsen et al., 2004; Okuda et al., 2019; Zhang et al., 2019]. The variation in the iron concentration within the mantle transition region may significantly contribute to the observed high-velocity anomalies in addition to the temperature effect of the cold subducting slab [Ringwood and Irifune, 1988; Y. Higo et al., 2006]. Thus, the properties of the bearing-Fe phase H under high pressure are important to understand the structure and composition of the mantle. It is well-known that the first-principles methods successfully simulate the Earth and planetary materials at high pressures and temperatures [Gillan et al., 2006; Wentzcovitch and Stixrude, 2010; Jahn and Kowalski, 2014]. This study calculated the crystal structure, elastic moduli, and seismic wave velocity of phase H with varying Fe concentrations (0, 12.5, 25, 100 at%) under 16–60 GPa by first-principles methods to understand the structure and composition of the mantle.

2. Simulations details

The First-principles simulation was performed using density functional theory (DFT) [Hohenberg and Kohn, 1964; Kohn and Sham, 1965] and the plane wave pseudopotential method, as implemented in the CASTEP codes [Clark, et al., 2005]. Ultrasoft pseudopotentials [Vanderbilt, 1990] were used to model electron–ion interactions with a plane-wave energy cutoff of 1000 eV. The generalized gradient approximation (GGA) with PBE parameterization [Perdew, et al., 1992] was used to describe exchange–correlation interactions. A convergence criterion of 5×10^{-7} a.u. for total energy was used in the self-consistent-field calculations. A $4 \times 6 \times 4$ Monkhorst Pack grid of k-points was adopted for sampling the Brillouin zone of the phase H unit cell with MgSiO_4H_2 , FeSiO_4H_2 , and AlAlO_4H_2 . Supercell were constructed for understanding the effect of different Fe contents (12.5 and 25at%). So K-points in those supercells are sampled by a different mesh, which is equivalent to that for the unit cell in reciprocal space. All structure parameters and atomic coordinates are fully relaxed to a static configuration (OK) and 16-60GPa using BFGS geometry optimization algorithms. The elastic constants were determined by stress-strain relations [Karki et al., 2001]. The magnitude of the applied strains was 0.01 and the linear relation was ensured to be enough for this strain range. For ferrous iron (Fe^{2+}) in this work, we consider the high spin ferromagnetic state (spin momentum $S=4/2$) during the calculation [Zhang and Oganov, 2006; Li et al., 2005; Hsu et al., 2011, 2012]. The benchmark calculations can be seen in the previous works [Liu et al., 2017, 2018].

3. Results

The Fe-bearing phase H structures were constructed by Tschermak substitution of Mg^{2+} by Fe^{2+} in the Mg end-member phase H. The three Fe-bearing phase H (FeSiO_4H_2 (Pure-Fe, 100at%), $\text{Mg}_{0.75}\text{Fe}_{0.25}\text{SiO}_4\text{H}_2$ (High-Fe, 25at%), and $\text{Mg}_{0.875}\text{Fe}_{0.125}\text{SiO}_4\text{H}_2$ (Low-Fe, 12.5at%)) were built and simulated in this work. The Mg end-member phase H (MgSiO_4H_2) (Pure-Mg) and Al end-member phase H ($\text{Al}_2\text{O}_4\text{H}_2$) (Pure-A) were cited from the previous works [Liu et al., 2017, 2018] for understanding the effect of Fe on the crystal structure and elastic properties.

3.1 Crystal structures of phase H under high pressure

The lattice constants of phase H under varying Fe concentrations are listed in Figure 1 and Table 1. For comparison, the results of pure-Al phase H are also provided in the Figure 1.

The lattice constants **a** and **b** of the pure-Al phase H are far smaller than those of the pure-Mg and Fe-bearing phase-H. However, the lattice constant **c** of the pure-Al phase H is higher than those of the other four phases. The values of **a** and **b** increase with an increase in the Fe concentration, although the value of **c** decreases. Compared to the results of pure-Mg phase H, the increase in the values of **a** and **b** of the phase H with 12.5, 25, and 100 at% Fe concentrations are 0.34% and 0.67%, 2.90% and 0.20%, and 0.38% and 1.58%, respectively. Also, the reduction in the value of **c** is 0.13%, 0.28%, and 2.66%, respectively, for the above Fe concentrations. Obviously, the effect of Fe on the value of **a** is maximum. The lattice constant differences between the pure-Al phase H and pure-Mg phase are

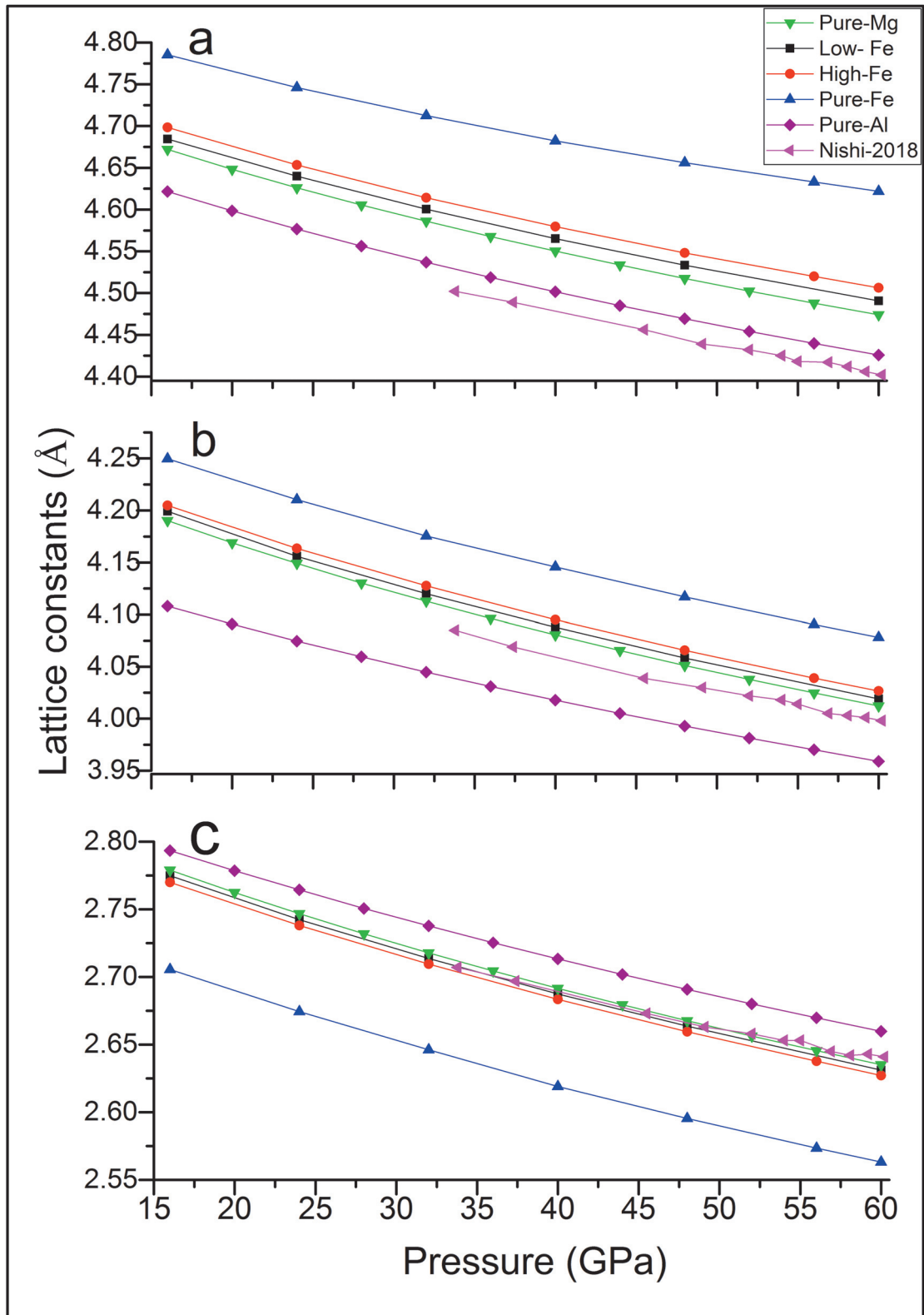


Figure 1. Figure 1 The lattice constants of the Phase H under high pressure.

P(GPa)	Cell parameters			Elastic property				
	a(Å)	b(Å)	c(Å)	Density(g/cm ³)	K(GPa)	G(GPa)	Vp(km/s)	Vs(km/s)
FeSiO ₄ H ₂ (100at% Fe)								
16	4.250	2.706	4.785	4.53	264.6	126.5	9.78	5.29
24	4.210	2.674	4.746	4.66	297.2	134.3	10.11	5.37
32	4.175	2.646	4.712	4.78	328.9	142.1	10.41	5.45
40	4.146	2.619	4.682	4.90	360.1	149.6	10.69	5.53
48	4.117	2.595	4.656	5.00	390.4	156.0	10.94	5.58
56	4.091	2.574	4.633	5.11	420.0	162.2	11.16	5.64
60	4.078	2.563	4.622	5.15	434.6	164.4	11.26	5.65
(Mg _{0.75} Fe _{0.25} SiO ₄ H ₂) (25at% Fe)								
16	4.205	2.770	4.698	3.84	249.8	135.1	10.59	5.93
24	4.164	2.738	4.653	3.96	280.4	143.3	10.92	6.02
32	4.128	2.709	4.614	4.07	309.7	151.0	11.21	6.10
40	4.095	2.683	4.580	4.17	338.6	159.0	11.49	6.18
48	4.066	2.660	4.548	4.26	368.1	166.0	11.76	6.24
60	4.027	2.627	4.506	4.40	408.9	175.1	12.08	6.31
Mg _{0.875} Fe _{0.125} SiO ₄ H ₂ (12.5at% Fe)								
16	4.199	2.775	4.685	3.72	245.3	142.0	10.80	6.18
24	4.156	2.742	4.640	3.84	276.8	151.0	11.15	6.27
32	4.120	2.714	4.600	3.95	306.9	158.6	11.45	6.34
40	4.088	2.687	4.565	4.05	335.9	166.2	11.73	6.41
48	4.058	2.664	4.533	4.15	364.3	173.1	11.98	6.46
60	4.019	2.631	4.491	4.28	405.6	182.3	12.31	6.53
MgSiO ₄ H ₂ (Pure-Mg)								
16	4.190	2.779	4.672	3.62	242.1	148.9	11.04	6.42
20	4.169	2.762	4.648	3.68	257.8	152.8	11.21	6.45
24	4.149	2.747	4.626	3.73			11.53	6.52
28	4.130	2.732	4.605	3.79	288.2	161.1	11.68	6.56
32	4.113	2.718	4.586	3.84	303.2	164.9	11.81	6.58
36	4.096	2.704	4.568	3.89	317.5	168.2	11.95	6.61
40	4.081	2.692	4.550	3.94	332.7	171.9	12.08	6.64
44	4.066	2.679	4.534	3.98	347.0	175.4	12.20	6.66
48	4.051	2.668	4.518	4.03	361.3	178.4	12.31	6.68
52	4.038	2.656	4.502	4.07	374.9	181.8	12.41	6.69
56	4.025	2.645	4.488	4.12	388.2	184.3	12.52	6.71
60	4.012	2.635	4.474	4.16	402.0	187.1	11.04	6.42
Al ₂ O ₄ H ₂ (Pure-Al)								
16	4.108	2.793	4.622	3.76	266.8	178.0	11.58	6.88
20	4.091	2.778	4.598	3.81	281.8	183.8	11.76	6.94
24	4.075	2.764	4.577	3.87	296.7	188.8	11.91	6.98
28	4.060	2.751	4.556	3.92	311.4	194.3	12.06	7.04
32	4.045	2.738	4.537	3.98	326.0	198.4	12.19	7.06
36	4.031	2.725	4.519	4.02	340.1	203.0	12.32	7.10
40	4.018	2.713	4.502	4.08	354.2	207.8	12.45	7.14
44	4.005	2.702	4.485	4.12	368.0	212.0	12.56	7.17
48	3.993	2.691	4.469	4.17	382.1	216.0	12.68	7.20
52	3.981	2.680	4.454	4.22	395.4	219.9	12.78	7.22
56	3.970	2.670	4.440	4.26	409.2	223.9	12.89	7.25
60	3.959	2.660	4.426	4.30	423.2	227.8	13.00	7.28

Table 1. The crystal and elastic properties of Phase H at high pressure.

1.6%, 1.07%, and 0.77% for *a*, *b*, and *c*, respectively. Thus, the effect of Al on the lattice constant is smaller compared to that of Fe. Nishi et al. [2018] measured the lattice constant of pure-Mg phase H using the multi-anvil apparatus under 300–1300K temperature and 34–60 GPa pressure. The comparative results at a temperature of 300K are listed in Figure 1. The calculated value of *c* is almost the same as the experimental result. However, the values of *a* and *b* are larger than those in the results as the use of GGA causes under-binding in the calculations. At the same time, the calculated changes in the lattice constants with pressure are consistent with the experimental results [Nishi et al., 2018].

3.2 Density

The densities of phase H are demonstrated in Figure 2 and Table 1. The densities of Fe-bearing and pure-Al phase H are larger than that of the pure-Mg phase H. The density increases with increasing Fe concentration. This is due to an increase in the total mass by the substitution of Mg with Fe atoms the rest is due to the smaller volume of the unit cell of Fe-bearing phase H. This is consistent with the previous result obtained for the effect of Fe on the density of the minerals [Yu et al., 2013; Liu et al., 2010]. The intrinsic mass difference between Mg and Fe gives a 3.3% density difference at the Fe concentrations of 12.5 at%, 7.7at%, 25 at%, 24.4at%, and 100at%. The density increment of pure-Al phase H is 3.8%. This effect is equivalent to that observed at the Fe concentration of 14.7 at%. The result indicates the greater effect of Fe on the density of phase H compared to Al.

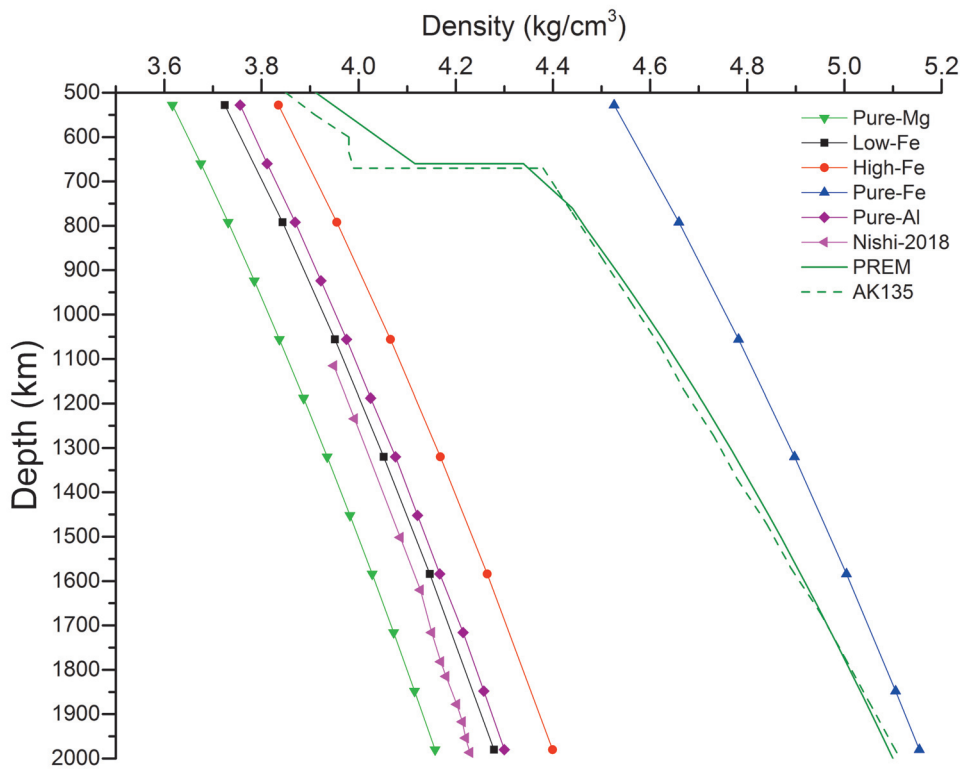


Figure 2. Density of Phase H and typical Earth’s density model PREM (Dziewonski and Anderson, 1981) and AK135 (Montagner and Kennett, 1995) indicate the mode of the Earth’s density.

Except for the pure-Fe phase H, the densities of the other phase H explored in this work are very lower than the density in the lower mantle. The density of the pure-Fe phase is the highest. The density of phase H containing enough Fe concentrations in different depths (the content of Fe is about 35.5–84.3 at%) would be very close to the mantle density. The results indicate that the existence of Fe-bearing phase H affects the structure of the mantle.

3.3 Elastic properties of phase H under high pressure

The knowledge of the elastic properties of mineral and rock is important to understanding the lithospheric flexure, onset of brittle failure, and earthquake source [Aki and Richards, 1980]. Also, the elastic parameter of the minerals and its dependence on pressure are crucial for understanding the structure and composition of the Earth's interior. The elastic constants of the four phase H (Pure-Fe, Pure-Mg, High-Fe, and Low-Fe phase) are shown in Figure 3. Phase H belongs to the P2/m space group symmetry. It has 13 independent elastic constants: C_{11} , C_{22} , C_{33} , C_{44} , C_{55} , C_{66} , C_{12} , C_{13} , C_{23} , C_{15} , C_{25} , C_{35} , and C_{46} . Except for C_{35} , all other constants linearly increase with pressure. The value of C_{35} decreases with increasing pressure, exhibiting negative values under the range of pressure studied in this work (16–60 GPa). The effects of Fe on the elastic constants are different. The values of C_{11} , C_{12} , C_{13} , C_{23} , and C_{25} increase with increasing Fe content, while those of C_{22} , C_{44} , C_{55} , C_{66} , C_{35} , and C_{46} decrease. The values of C_{33} and C_{15} were the highest for pure-Fe phase H. These constants decrease with increasing Fe concentration for the other three phases.

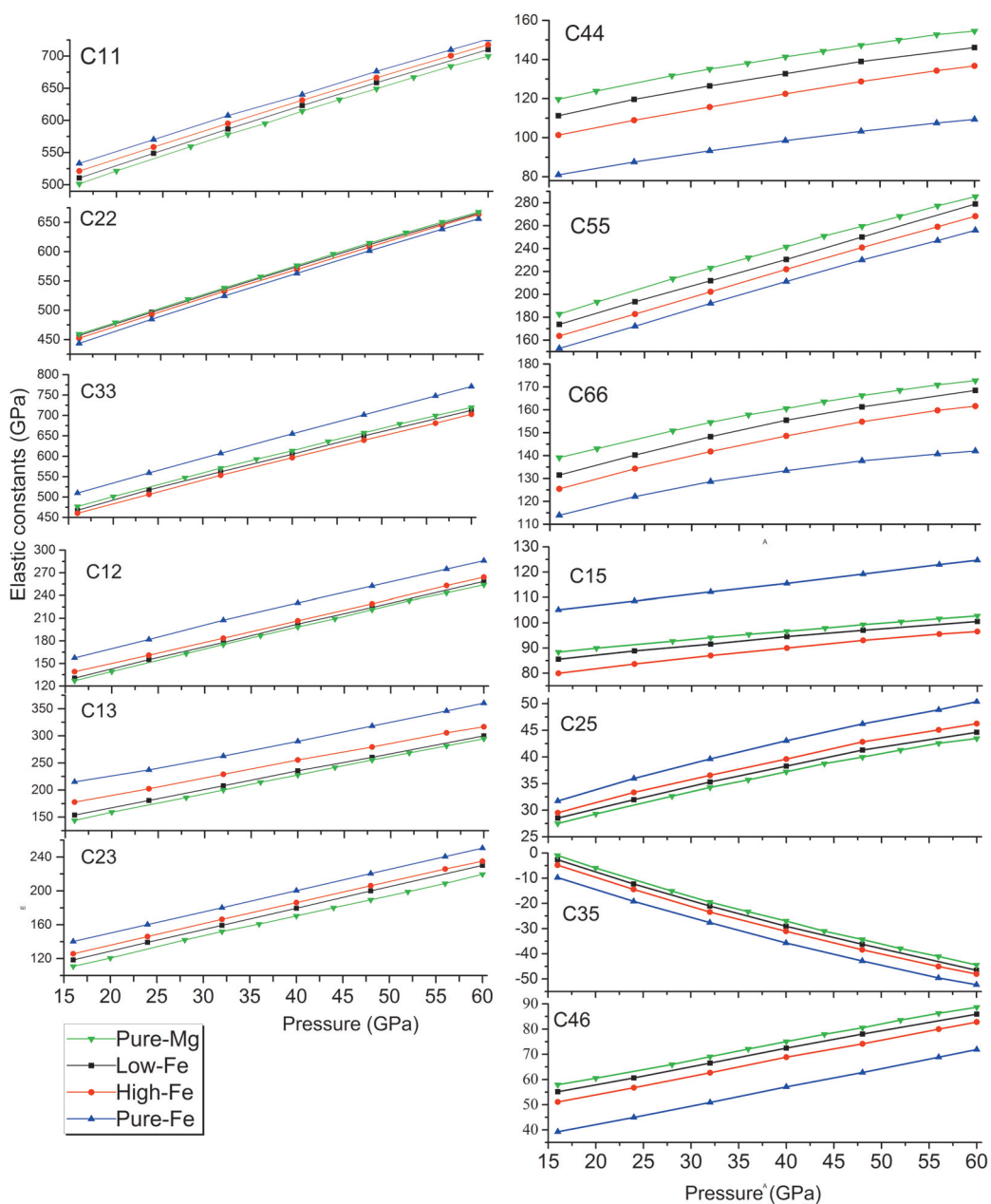


Figure 3. The elastic constants of bearing-Fe Phase H.

Structure and elasticity of Fe-bearing Phase H

Figure 4 and Table 1 show the change in the bulk modulus (K) and shear modulus (G) of phase H with pressure and Fe concentration. The pure-Al phase H has the largest G value among the five phases. The value of K for phase H increases with increasing Fe concentration while G decreases. The differences in the elastic properties of FeO_6 and MgO_6 octahedra lead to a change in the values of bulk and shear moduli for pure-Mg phase H and Fe-bearing phase H. According to the bulk modulus-volume systematics of the cation-anion polyhedra [Hazen and Finger, 1979], the bulk modulus of the Fe-bearing minerals increases with Fe concentration, which is demonstrated in this work. The results are in accordance with the ultrasonic experimental and first-principles simulated data for the effects of Fe on olivine, ringwoodite [Higo et al., 2006], and wadsleyite [Hazen et al., 2000; Liu et al., 2009] at high pressures. Nishi et al. [2018] presented the value of K for pure-Mg phase H to be 344.6 GPa at a pressure of 35 GPa. Tsuchiya and Mookherjee [2015] found that the K value is 328 GPa at a pressure of 36 GPa by GGA-DFT simulation. The value of K for pure-Mg phase H in this work was found to be 317.5 GPa at a pressure of 36 GPa. The values obtained from the present and previous studies [Tsuchiya and Mookherjee, 2015] are slightly lower than the experimental result due to the under-binding effect resulting from the GGA-DFT simulation.

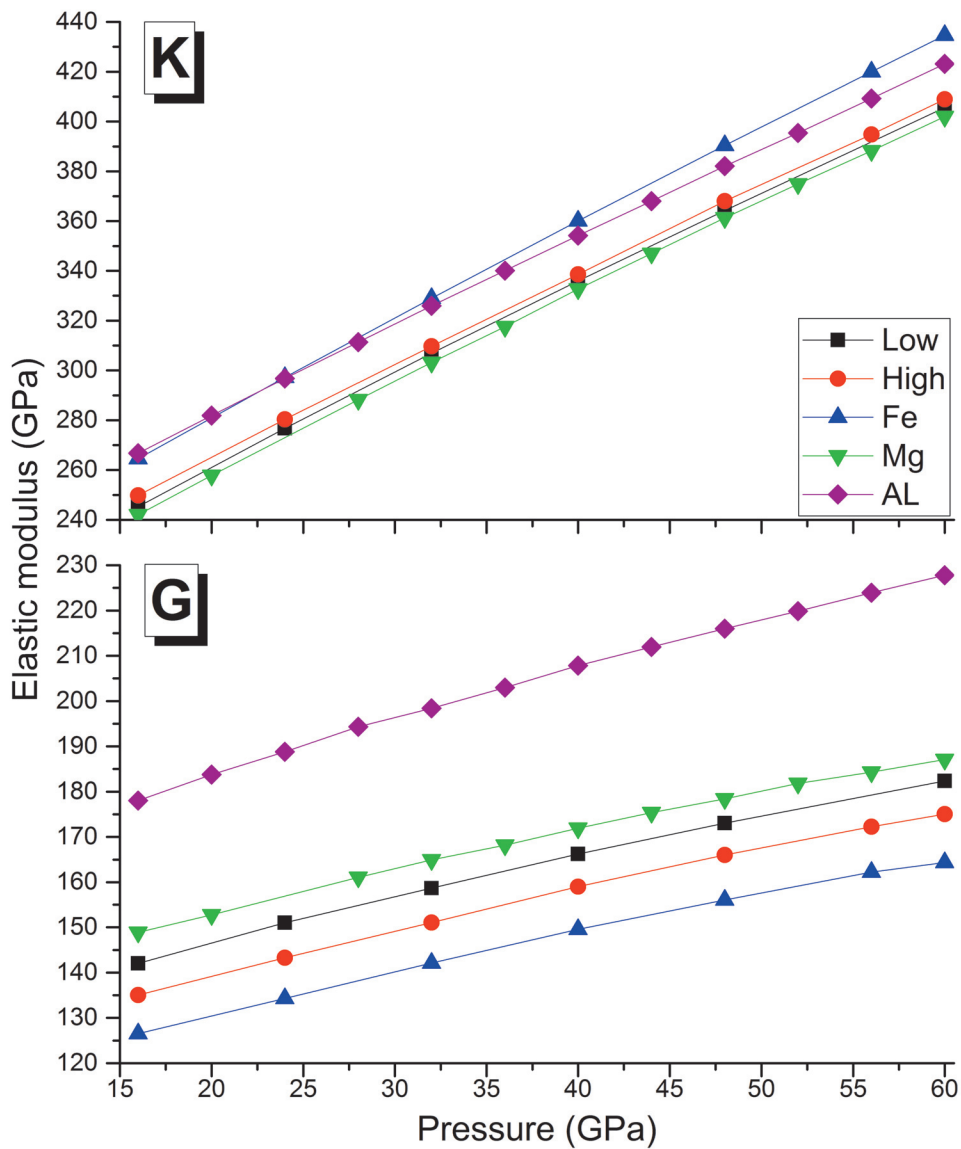


Figure 4. The elastic modulus of the Phase H.

The values of K_0 , G_0 , and pressure derivatives of K and G (K' and G') were calculated by linear fitting the change in the values of K and G of the phase H with increasing pressure. The values of K_0 are 185.9, 189, 193, 204.4, and 211.7 GPa, and that of G_0 are 136.1, 128.7, 121.4, 113.6, and 161.9 GPa, respectively for pure-Mg, low-Fe, high-Fe, pure-Fe and pure-Al phase H. The values of K' are 3.63, 3.64, 3.61, 3.86, and 3.54, and that of G' are 0.87, 0.97, 0.91, 0.87, and 1.12 for pure-Mg, low-Fe, high-Fe, pure-Fe, and pure-Al phase H, respectively. The pure-Mg and Fe-bearing phase H have similar values for K' and G' . However, they are different from the elastic moduli of pure-Al phase H. Nishi et al. (2018) found the K_0 of pure-Mg phase H to be 204 GPa for the fixed value of $K' = 4$, and 167 GPa for $K' = 5$ by fitting the third-order Birch-Murnaghan equation of state. The GGA-DFT calculation [Tsuchiya and Mookherjee, 2015] returned the values of K_0 and K' of the pure-Mg phase H to be 147GPa and 4.9, respectively. The calculated K_0 value in this study is exactly between the experimental results, although larger than the previous GGA-DFT calculation. The value of K for the pure-Al phase H was found to be 219GPa at the fixed value of $K' = 4$ using the high-pressure experiment by San-FuruKawa et al. [2009], which is very close to the value of 211.7GPa obtained in this work.

The wave velocities obtained from seismic observations, experimentation, and calculations reflect the composition and structure of the Earth. Based on the mass densities and elastic moduli, the compressional (V_p) and shear (V_s) wave velocities of phase H were calculated. The wave velocities of phase H under pressure are plotted along with the typical velocity structure of the Earth in Figure 5 and Table 1. The V_p and V_s values increase almost linearly with pressure. The pure-Al phase H has the highest values for V_p and V_s among the five phases, attributing to its high elastic modulus and low density., The values of V_p and V_s for the other four phases decrease with increasing Fe concentration. Compared to the wave velocity of pure-Mg phase H, the value of V_p for the phase H containing 12.5, 25, and 100 at% Fe decreases by 1.9%, 3.8%, and 6.9%, respectively, while that of V_s decreases by 3.2, 6.7, and 9.9%, respectively. However, the values of V_p and V_s for the pure-Al phase increase by 4.3% and 8.0%, respectively. The change in wave velocity is attributed to the increase in density caused by the presence of iron in Fe-bearing phase H, and an increase in the values of K and G in pure-Al phase H.

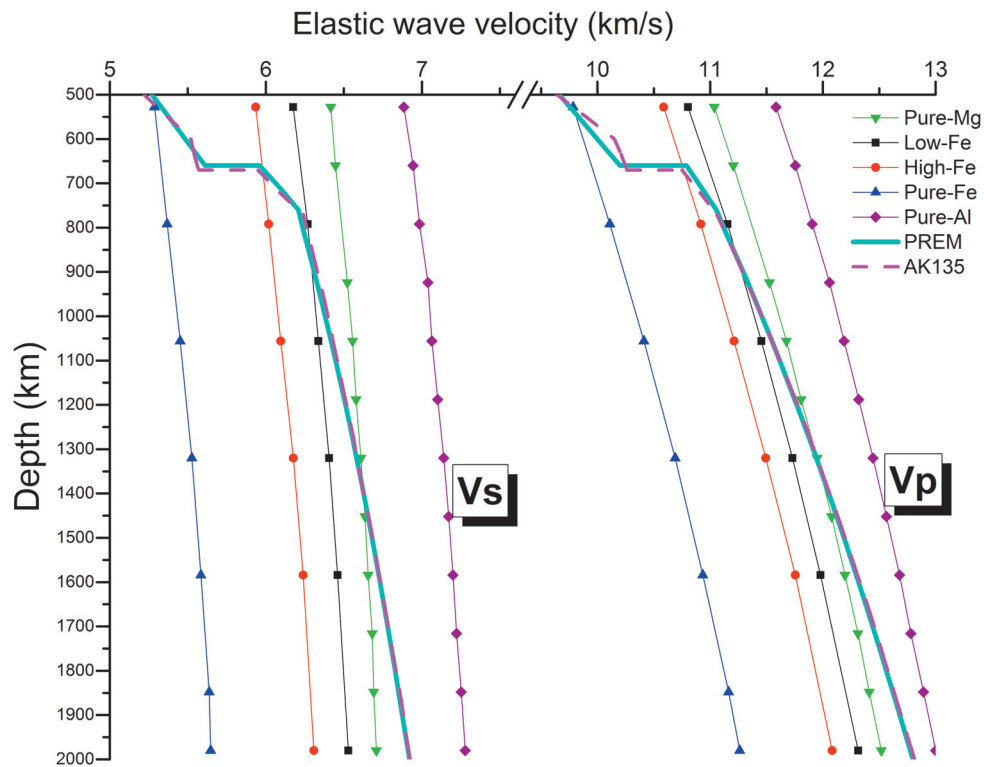


Figure 5. Wave velocities of phase H and the typical density model of the Earth PREM [Dziewonski and Anderson, 1981] and AK135 [Montagner and Kennett, 1995] indicate the mode of the wave velocity of the Earth.

The wave velocity of pure-Al phase H is higher than that of the typical velocity structure of the Earth throughout the range of depths explored in this study. The wave velocities of pure-Mg and Fe-bearing phase H are close to the Earth's typical velocity at the depths of 500–1400 km, which gradually decrease above 1400 km. The differences in the wave velocities for phase H with varying concentrations of Mg, Fe, and Al are useful for understanding the velocity structure and composition of the mantle. For instance, it may be inferred that the chemical heterogeneity, such as Fe-rich hydrous minerals, may be responsible for the formation of low-velocity zones in the mantle or other layers in the interior of the Earth. Thompson et al. [2017] showed that the iron-enriched solid solutions from the FeOOH-AlOOH-MgSiH₂O₄ system contributed to the observed seismic properties of large low-shear velocity provinces (LLSVP) in the Earth's lower mantle. It is concluded from the results of this study that the FeOOH-AlOOH-MgSiH₂O₄-FeSiH₂O₄ system is responsible for the observed seismic properties of LLSVP in the Earth's lower mantle.

4. Discussions

Phase D (MgSi₂O₆H₂) was discovered as a dissociation product of serpentine at pressures above 20 GPa [Liu, 1987]. It has been considered as the most thermodynamically stable phase under the lower mantle conditions [Frost et al., 1998; Shieh et al., 1998]. It was discovered that phase D transforms into phase H at 44 GPa [Nishi et al., 2014]. Antigorite was found to transform the phase assemblage, including phase H, at pressures above 35–40 GPa corresponding to those in the upper part of the lower mantle [Nishi et al., 2015]. Therefore, phase H is an important mineral in the deep Earth. It was experimentally found that the Fe-bearing bridgmanite ((Mg_{0.85}Fe_{0.15})SiO₃) loses Fe and disproportionate to a nearly Fe-free MgSiO₃ bridgmanite and an Fe-rich phase H at 95–101 GPa pressure and 2200–2400 K temperature [Zhang et al., 2014]. The spin transition of Fe in ferropericlae (Mg_{0.83}Fe_{0.17})O at high pressures has profound implications on the structure and transport properties of the Earth's lowermost mantle [Badro et al., 2003]. The high-pressure experiments showed that Fe²⁺ ions in the deep magma ocean disproportionate to form Fe³⁺ ions and metallic iron at high pressures. The reduced iron (metallic iron) sinks to the core and leaves an oxidized mantle that leads to the degasification of carbon dioxide and water from the mantle [Armstrong et al., 2019]. Therefore, the concentration and state of Fe in phase H have important impacts on the structure and composition of the mantle and atmosphere. The quantitative effects of Fe on the density, elastic moduli (K and G), and wave velocities (V_p and V_s) of phase H were calculated and presented in Figure 6. The effects of Fe concentration on the density and value of K show an excellent linear relationship. There is a quadratic relationship between the concentration of Fe and the values of V_p and V_s. The effect of Fe concentration on the value of G varies accordingly. The fitted equations for the changes in the density, elastic moduli (K and G), and wave velocities (V_p and V_s) of phase H with Fe concentration are shown in Figure 6. The wave velocities from the seismic and geophysical observations reflect the structure of the Earth. Being one of the most important components of the mantle, the quantitative equations for the effects of Fe concentration from this study combined with the results from seismic and geophysical observations could provide information about the concentration of Fe in the deep Earth. This can be used to understand the role of Fe on the evolution of the Earth. For example, the Earth's density mode shows that phase H containing 35.5–84.3 at% concentrations of Fe has a similar density to that of the mantle at different depths of the Earth. The formation energy (the enthalpy equal to the total energy at 0 K) of phase H containing 12.5, 25, and 100 at% Fe were calculated at 0 GPa to evaluate the formation of (Fe, Mg)SiO₄H₂ solution by the substitution of Mg with Fe. The values were found to be 14.066 eV, 28.193 eV, and 112.581 eV, respectively. The formation energy linearly increases with Fe concentration. The fitting equation can be described as Formation energy, E = 1.126 Fe% (E in eV, and Fe% in at%). The result shows that the formation of a solid solution of Fe-bearing phase H becomes difficult with increasing Fe concentration.

Perhaps, it is not enough to consider the properties of materials at zero temperature to resolve most of the problems in the Earth and planetary sciences. The elasticity depends on the structure, pressure, temperature, and chemical composition. The elastic coefficients increase at most by a factor of five over the entire mantle pressure regime. However, the experimental or theoretical determination of the mineral properties at simultaneous pressure and temperature conditions in the geophysical magnitudes is still challenging. However, it is seen that the effects of temperature on the seismic observable physical properties of the material (density and wave velocities) are monotonically suppressed with increasing pressure [Karki, 1999, 2015]. Therefore, the properties of phase H are calculated under high pressure in this work. The effect of temperature on the elasticity of phase H was inferred on

the basis of earlier studies [Wentzcovitch et al., 2010; Karki et al., 1999; Sinogeikin et al., 2003]. Wentzcovitch et al. [2010] evaluated the thermoelastic properties of MgSiO_3 perovskite at high pressure and temperature using the first principles methods and quasi-harmonic calculations. Also, the pressure and temperature derivatives of K , G , V_p , and V_s ($\partial G/\partial P$, $\partial K_s/\partial P$, $\partial V_p/\partial P$, $\partial V_s/\partial P$ and $\partial G/\partial T$, $\partial K/\partial T$, $\partial V_p/\partial T$, $\partial V_s/\partial T$) were determined to be 4.8, 2.0, 0.06 km/s/GPa, 0.026 km/s/GPa, and -0.021 , -0.026 , -0.0003 km/s/K, -0.0002 km/s/K, respectively. The pressure and temperature derivatives for K and G for MgO [Karki et al., 1999], an important component of the lower mantle, were found to be 4.15, 2.44, and -0.015 , -0.0216 , respectively. The temperature derivatives of K , G , V_p , and V_s for the Fe-bearing ringwoodite $(\text{Mg}_{0.91}\text{Fe}_{0.09})_2\text{SiO}_4$ [Sinogeikin et al., 2003] were -0.021 GPa/K, -0.016 GPa/K, 0.00056 km/s/K, and 0.0004 km/s/K, respectively.

Considering the effect of temperature on the seismic velocity of MgSiO_3 perovskite and Fe-bearing ringwoodite $(\text{Mg}_{0.91}\text{Fe}_{0.09})_2\text{SiO}_4$, the typical minerals of the deep Earth, it is seen that a temperature of 2000K. The temperature at 500–2000 km depths of the Earth is about 1800–2500K [Katsura, et al., 2010] on phase H leads to decrease of its seismic velocity in 0.4–1.2 km/s. The change in the seismic velocity of phase H caused by the temperature is less than 10%. Thus, the depth of phase H in the Earth reduces with temperature, which creates the demand for a higher concentration of Fe to match the mantle density profile. The specific effect of temperature on the properties of phase H would be evaluated in future works.

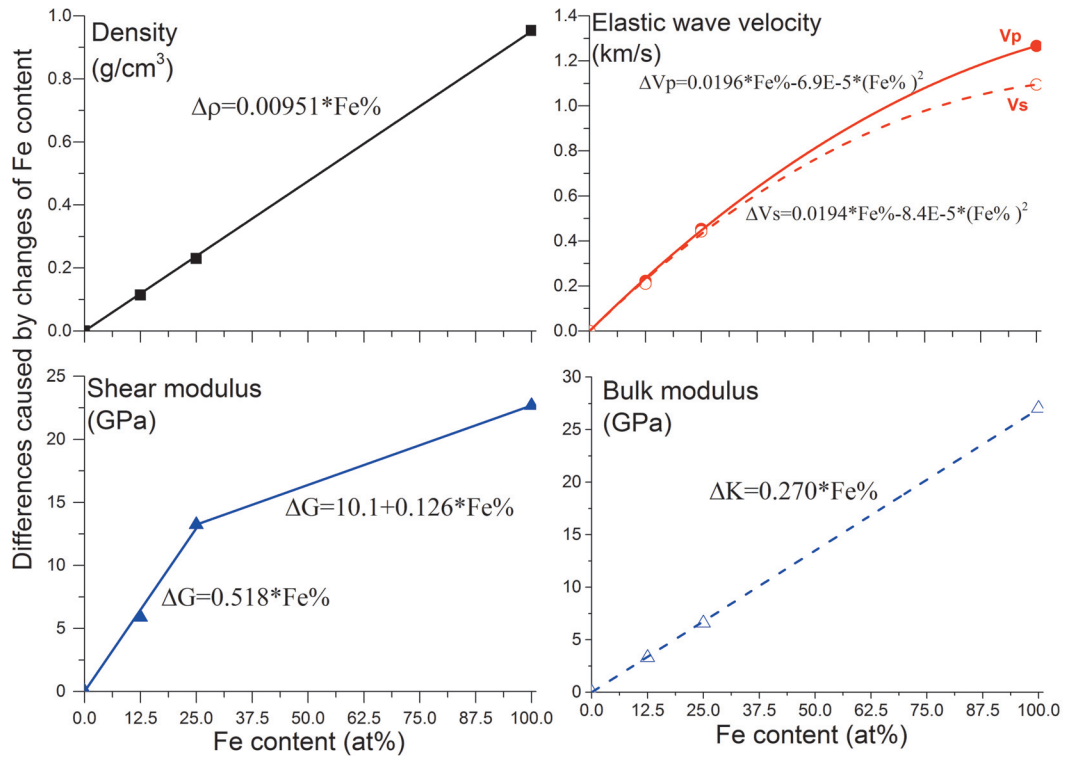


Figure 6. The changes of properties of phase H with Fe content. (The fitted formulas of effect of Fe content also list in the picture).

5. Conclusion

The crystal structure and elastic properties of phase H containing different Fe concentrations were calculated by the first-principles method to study the effect of Fe on minerals. The lattice constants a and b increase with Fe concentration, while the value of c decreases. Among the three lattice constants, the effect of Fe is predominant in a . The density of phase H linearly increases with Fe concentration. Except for the pure-Fe phase, the densities of

the other phases are far lower than the lower mantle density structure. The phase H containing 35.5–84.3 at% Fe meets the mantle density model at different depths of the Earth.

The effects of Fe on the elastic constants show varying tendencies. The value of K for phase H increases with increasing Fe concentration, while that of G decreases. The result is in accordance with the general effect of Fe on the elastic properties of the mineral. The values of V_p and V_s of the phase H rise almost linearly with increasing pressure. The values of V_p and V_s decrease with increasing Fe concentration. The wave velocities of pure-Mg phase H and Fe-bearing phase H are close to the Earth's typical velocity at the depths of 500–1400 km. The FeOOH- AlOOH - MgSiH_2O_4 - FeSiH_2O_4 system is responsible for the observed seismic properties of LLSVP in the Earth's lower mantle. The quantitative effects of Fe on the density, elastic moduli (K and G), and wave velocities (V_p and V_s) of phase H were calculated and listed as fitted equations. These results can be used to infer the Fe concentration and structure of the deep Earth. However, further studies are needed to understand the effects of the concentrations of Fe and Al, and temperature on the properties of the mineral at high pressure and temperature. This work focused on the effect of Fe^{2+} and the effect of Fe^{3+} and its spin transition under high pressures shall be studied in the future to completely understand the structure and composition of the mantle.

Acknowledgements. This work was supported by the Foundation of the Key Laboratory of Earthquake Forecasting, the Institute of Earthquake Forecasting, CEA (Grant No. 2019IEF0101-1, 2019IEF0502, 2017KLEP03) and by two projects of National Natural Science Foundation of China 41762008 and 42072094..

References

- Aki, K., P.G. Richards (1980). *Quantitative Seismology: Theory and Methods*, vol. 2, W. H. Freeman, New York.
- Armstrong, K., C.A. McCammon, D.C. Rubie, T.B. Ballaran (2019). Deep magma ocean formation set the oxidation state of Earth's mantle, *Science*, 365 (6456), 903-906.
- Clark, S. J., M.D. Segall, C. J. Pickard, P. J. Hasnip, M.I.J. Probert, K. Refson, M.C. Payne (2005). First principle methods using CASTEP, *Zeitschrift für Kristallographie*, 220, 567-570.
- Dziewonski, A.M., D.L. Anderson (1981). Preliminary Reference Earth Model (PREM), *Phys. Earth Planet. Inter.* 25, 297-356.
- Frost, D.J., Y.W. Fei (1998). Stability of phase D at high pressure and high temperature, *J. Geophys. Res.: Solid Earth*, 103(B4), 7463-7474.
- Ganskow, G., T.B. Ballaran, F. Langenhorst (2010). Effect of iron on the compressibility of hydrous ringwoodite, *Am. Mineral.* 95, 747-753.
- Ghosh, S., M.W. Schmidt (2014). Melting of phase D in the lower mantle and implications for recycling and storage of H_2O in the deep mantle, *Geochim. Cosmochim. Acta.* 145, 72-88.
- Gillan, M.J., Alfe, D., J. Brodholt, L. Vocadlo, G.D. Price (2006). First principles modelling of earth and planetary materials at high pressures and temperatures, *Rep. Prog. Phys.* 69, 2365-2441.
- Hazen, R.M., L.W. Finger (1979). Bulk modulus-volume relationship for cation-anion polyhedral, *J. Geophys. Res.* 84, 6723-6728.
- Hazen, R.M., M.B. Weinberger, H. Yang, C.T. Prewitt (2000). Comparative high pressure crystal chemistry of wadsleyite, β - $(\text{Mg}_{1-x}\text{Fe}_x)_2\text{SiO}_4$, with $x=0$ and 0.25, *Am Mineral.* 85, 770-777.
- Higo, Y., T. Inoue, B. Li, T. Irifune, R. Liebermann (2006). The effect of iron on the elastic properties of ringwoodite at high pressure, *Phys. Earth Planet. Inter.* 159, 276-285.
- Hohenberg, P., W. Kohn, (1964). Inhomogeneous electron gas. *Phys. Rev. B* 136, 864-871.
- Hsu, H., P. Blaha, M. Cococcioni, R. Wentzcovitch (2011). Spin-state crossover and hyperfine interactions of ferric iron in MgSiO_3 perovskite, *Phys. Rev. Lett.* 106 (11), 118501.
- Hsu, H., Y.G. Yu, R.M. Wentzcovitch (2012). Spin crossover of iron in aluminous MgSiO_3 perovskite and post-perovskite, *Earth Planet. Sci. Lett.*, 359-60, 34-39.
- Jacobsen, S.D., J.R. Smyth, H. Spetzler, C.M. Holl, D.J. Frost (2004). Sound velocities and elastic constants of iron bearing hydrous ringwoodite, *Phys. Earth Planet Inter.*, 143, 47-56.
- Jahn, S., P. Kowalski (2014). Theoretical approaches to structure and spectroscopy of earth materials, *Rev. Miner.*

- Geochem., 78.
- Karki, B. B., L. Stixrude, R. M. Wentzcovitch (2001). High-pressure elastic properties of major materials of earth's mantle from first principles, *Rev. Geophys.*, 39, 507-534.
- Karki, B.B. (2015). First-principles computation of mantle materials in crystalline and amorphous phases, *Phys. Earth Planet. Inter.* 240, 43–69.
- Karki, B. B., R. M. Wentzcovitch, S. de Gironcoli, S. Baroni (1999). First-principles determination of elastic anisotropy and wave velocities of MgO at lower mantle conditions, *Science*, 286, 1705-1707.
- Katsura, T., A. Yoneda, D. Yamazaki, T. Yoshino, E. Ito (2010). Adiabatic temperature profile in the mantle, *Phys. Earth Planet. Inter.*, 183, 212–218.
- Kohn, W., L.J. Sham (1965). Self-consistent equations including exchange and correlation effects, *Phys. Rev. A*, 140, 1133-1138.
- Li, L., J.P. Brodholt, S. Stackhouse, D.J. Weidner, M. Alfredsson, G.D. Price (2005). Electronic spin state of ferric iron in Al-bearing perovskite in the lower mantle, *Geophys. Res. Lett.*, 32 (17), L17307.
- Liu, G., L. Liu, L. Yang, L. Yi, H. Liu, Y. Gao, C. Zhuang, S. Li (2018). Crystal structure and elasticity of Al-bearing phase H under high pressure, *AIP Advances* 8, 055219.
- Liu, L., J.G. Du, W. Liu, J.J. Zhao, H. Liu (2010). Elastic behavior of $(\text{Mg}_x\text{Fe}_{1-x})_2\text{SiO}_4$ olivine at high pressure from first-principles simulations, *J. Phys. Chem. Solids*, 71, 1094-1097.
- Liu, L.G. (1987). Effects of H_2O on the phase behaviour of the forsterite-enstatite system at high pressures and temperatures and implications for the Earth Physics, *Earth Planet. Inter.*, 49(1-2), 142-167.
- Liu, W., J. Kung, B. Li, N. Nishiyama, Y. Wang (2009). Elasticity of $(\text{Mg}_{0.87}\text{Fe}_{0.13})_2\text{SiO}_4$ wadsleyite to 12GPa and 1073K, *Phys. Earth Planet. Inter.*, 174, 98-104.
- Lv, C., L. Liu, Y. Gao, H. Liu, L. Yi, C. Zhuang, Y. Li, J. Du (2017). Structural, elastic, and vibrational properties of phase H: A first-principles simulation, *Chin. Phys. B*, 26(6): 06740.
- Montagner J.P., B.L.N. Kennett (1995). How to reconcile body-wave and normal-mode reference Earth models?, *Geophys. J. Int.*, 125, 229-248.
- Nishi, M., T. Irifune, S. Greaux, Y. Tange, Y. Higo (2015). Phase transitions of serpentine in the lower mantle, *Phys. Earth Planet. Inter.*, 245, 52-58.
- Nishi, M., T. Irifune, J. Tsuchiya, Y. Tange, Y. Nishihara, K. Fujino, Y. Higo (2014). Stability of hydrous silicate at high pressures and water transport to the deep lower mantle, *Nature Geoscience*, 7, 224-227.
- Nishi, M., J. Tsuchiya, T. Arimoto, S. Kakizawa, T. Kunimoto, Y. Tange, Y. Higo, T. Irifune (2018). Thermal equation of state of MgSiO_4H_2 phase H determined by in situ X-ray diffraction and a multianvil apparatus, *Phys. Chem. Miner.*, 45, 995-1001.
- Nishi, M., J. Tsuchiya, Y. Kuwayama, T. Arimoto, Y. Tange, Y. Higo, T. Hatakeyama, T. Irifune (2019). Solid solution and compression behavior of hydroxides in the lower mantle, *J. Geophys. Res.*, 124(10), 10231-10239.
- Ohtani, E., Y. Amaike, S. Kamada, T. Sakamaki, N. Hirao (2014). Stability of hydrous phase H MgSiO_4H_2 under lower mantle conditions, *Geophys. Res. Lett.* 41 (23), 8283-8287.
- Okuda, Y., K. Ohta, R. Sinmyo, K. Takashi, Y. Ohishi (2019). Effect of spin transition of iron on the thermal conductivity of (Fe, Al)-bearing bridgmanite, *Earth Planet. Sci. Lett.*, 520, 188-198.
- Perdew, J. P., J. A. Chevary, S. H. Vosko, K. J. Johnson, A. R. Jackson, M. R. Pederson, D. J. Singh, and Carlos Fiolhais (1992). Atoms, molecules, solids, and surfaces: Applications of the generalized gradient approximation for exchange and correlation, *Phys. Rev. B*, 46, 6671-6687.
- Ringwood, A.E., T. Irifune (1988). Nature of the 650-km seismic discontinuity: implications for mantle dynamics and differentiation, *Nature*, 331, 131-136.
- Sano-Furukawa, A., H. Kagi, T. Nagai, S. Nakano, S. Fukura, D. Ushijima, R. Iizuka, E. Ohtani, T. Yagi (2009). Change in compressibility of δ -AlOOH and δ -AlOOD at high pressure: a study of isotope effect and hydrogen-bond symmetrization, *Am. Miner.*, 94, 1255-1261.
- Shieh, S.R., H.K. Mao, R.J. Hemley (1998). Decomposition of phase D in the lower mantle and the fate of dense hydrous silicates in subducting slabs, *Earth Planet. Sci. Lett.*, 159.1: 13-23.
- Sinogeikin, S. V., J. D. Bass, T. Katsura (2003). Single-crystal elasticity of ringwoodite to high pressures and high temperatures: implications for 520 km seismic discontinuity, *Phys. Earth Planet. Inter.*, 136, 41-66.
- Struzhkin, V., G. Vankó, G. Monaco (2003). Iron Partitioning in Earth's Mantle: Toward a Deep Lower Mantle Discontinuity, *Science*, 300 (5620), 789-791.

Structure and elasticity of Fe-bearing Phase H

- Thompson, E. C., A. J. Campbell, J. Tsuchiya (2017). Elasticity of ϵ -FeOOH: Seismic implications for Earth's lower mantle, *J. Geophys. Res. Solid Earth*, 122.
- Tsuchiya, J., M. Mookherjee (2015). Crystal structure, equation of state, and elasticity of phase H (MgSiO_4H_2) at Earth's lower mantle pressures, *Sci. Rep.*, 5, 5534.
- Tsuchiya, J., T. Tsuchiya, (2009). First principles investigation of the structural and elastic properties of hydrous wadsleyite under pressure, *J. Geophys. Res.*, 114, B02206.
- Vanderbilt, D. (1990). Soft self-consistent pseudopotentials in a generalized eigenvalue formalism, *Phys. Rev. B*, 41, 7892-7895.
- Wentzcovitch, R. M., B. B. Karki, M. Cococcioni, S. de Gironcoli (2004). Thermoelastic properties of MgSiO_3 -perovskite: Insights on the nature of the Earth's lower mantle, *Phys. Rev. Lett.*, 92, 018501-4.
- Wentzcovitch, R., L. Stixrude (2010). Theoretical and computational methods in mineral physics: geophysical applications, *Rev. Miner. Geochem*, 71.
- Yu, Y.G., V.L. Vinograd, B. Winkler, R.M. Wentzcovitch (2013). Phase equilibria of $(\text{Mg,Fe})_2\text{SiO}_4$ at the Earth's upper mantle conditions from first-principles studies, *Phys. Earth Planet. Inter.* 217, 36-47.
- Zhang, F., A.R. Oganov (2006). Valence state and spin transitions of iron in Earth's mantle silicates, *Earth Planet. Sci. Lett.*, 249 (3-4), 436-443.
- Zhang, L., Y. Meng, W. Yang, L. Wang, W.L Mao, Q-S. Zenge, J.S. Jeong, A.J. Wagnert al., (2014). Disproportionation of $(\text{Mg,Fe})\text{SiO}_3$ perovskite in Earth's deep lower mantle, *Science*, 344(6186), 877-882.
- Zhang, Y., Yoshino, T., Yoneda, A., M. Osako (2019). Effect of iron content on thermal conductivity of olivine with implications for cooling history of rocky planets, *Earth Planet. Sci. Lett.* 519, 109-119.

***CORRESPONDING AUTHOR: Chunqiang ZHUANG,**

Institute of Microstructure and Property of Advanced Materials,
Beijing Key Lab of Microstructure and Property of Advanced Materials,
Beijing University of Technology, Beijing100124, China
e-mail: chunqiang.zhuang@bjut.edu.cn

© 2020 the Istituto Nazionale di Geofisica e Vulcanologia.

All rights reserved